Biosensors and Bioelectronics 82 (2016) 32–39

Contents lists available at ScienceDirect

Biosensors and Bioelectronics

journal homepage: www.elsevier.com/locate/bios

Toehold enabling stem-loop inspired hemiduplex probe with enhanced sensitivity and sequence-specific detection of tumor DNA in serum

Fan Yang [1], Siqi Wang [1], Yulin Zhang, Lina Tang, Dan Jin, Yong Ning *, Guo-Jun Zhang *

School of Laboratory Medicine, Hubei University of Chinese Medicine, 1 Huangjia Lake West Road, Wuhan 430065, China

ARTICLE INFO

Article history:
Received 26 January 2016
Received in revised form
8 March 2016
Accepted 21 March 2016
Available online 23 March 2016

Keywords:
Electrochemical DNA sensor
Stem-loop structure
Toehold
Exonuclease III
Tumor DNA

ABSTRACT

The sensitivity of structure-switchable electrochemical DNA (E-DNA) sensors is generally limited by the irremovable redox labels that are close to or distant from the sensing interface. To address this issue, we design a semiduplex probe inspired by the stem-loop structure, in which the "nicked loop" domain can serve as toehold to mediate a target-responsive strand-displacement reaction. Such a reaction can fundamentally eliminate the post-responsive background current that arises from the irremovable probe, and thus improve the sensitivity. This novel toehold E-DNA (tE-DNA) sensor is able to achieve a detection limit as low as 0.2 pM, which is lower than that of the classic stem-loop structured sensor by two orders of magnitude. Moreover, the toehold domain endows the sensor an excellent selectivity against a single-base mismatched sequence and high binding kinetics. By combining this heterogeneous surface-based dynamic self-assembly design with a homogeneous enzyme amplification strategy, the sensitivity can be further improved by three orders of magnitude to sub-femtomolar level. Additionally, this unique biosensor presents reliable reusability, and is capable of probing low abundance of target DNA directly in complex matrices, such as human serum, with minimal interference. These advantages make our tE-DNA sensor a promising contender in the E-DNA sensor family for clinical diagnostics.

1. Introduction

It is highly necessary to tailor-engineer a sensitive, selective and low-cost biosensing means for nucleic acids assay, considering the ever-increasing clinical expectation for rapid and early diagnosis of cancer and infectious diseases (Hsieh et al., 2015; Giljohann and Mirkin, 2009). On the basis of precise Watson-Crick pairing principle, a variety of nucleic acid bioassays have been demonstrated (Wang et al., 2012; Chung et al., 2013; Liong et al., 2013). However, either the slow readout or the bulk probing component makes them incompatible with point-of-care testing. To overcome this hurdle, several functional micro- and nanostructured DNA biosensing devices, including platforms based on microfluidics (Hong et al., 2004; Ferguson et al., 2011), nanoplasmonics (Anker et al., 2008; Tokel et al., 2014), nanomechanics (Lu et al., 2011) and field-effect transistor (FET) (Cai et al., 2014; Cai et al., 2015; Yang and Zhang, 2014), have been exploited to perform rapid and ultrasensitive DNA quantification in multicomponent settings. Nevertheless, most, if not all, of these methods suffer from either high fabrication cost or complicated photolithography procedures. In contrast, the electrochemical DNA (E-DNA) sensor has unique appeal in point-of-care diagnostics and practical clinical monitoring, because of its intrinsic sensitive, simple, portable and inexpensive attributes (Drummond et al., 2003; Fan et al., 2003). Moreover, the electrochemical sensing interface is compatible with advanced micro- and nanofabrication technology as well as functional nanomaterials, and the combination can significantly enhance the sensor's response to the target sequence by maximizing mutual advantages (Zhu et al., 2014; Zhang et al., 2007; Ferguson et al., 2009; Soleymani et al., 2009). The performance, however, stringently depends on perfect and rational cooperation between the sensing elements, which is hard to control. Therefore, how to construct a simple and highly sensitive E-DNA sensor is a pressing issue.

To this end, a hairpin structured E-DNA sensor has been created, which comprises a redox-tagged conformation-switchable stem-loop probe assembled on an interrogating gold electrode (Fan et al., 2003). Following this structurally switchable sensing mechanism, a family of "signal-off" or "signal-on" E-DNA sensors

* Corresponding author.
E-mail addresses: ningyong128@163.com (Y. Ning), zhanggj@hbtcm.edu.cn (G.-J. Zhang).
[1] These authors contributed equally to this work.

http://dx.doi.org/10.1016/j.bios.2016.03.054
0956-5663/

has been engineered. These sensors feature reagentless, and are compatible with on-site diagnostics (Xiao et al., 2005; 2006; 2007a, 2007b; Ricci et al., 2007; Lubin and Plaxco, 2010; Wu and Lai, 2013, 2014; Idili et al., 2014). However, the covalently attached terminal redox label is irremovable in these conformation-switchable signaling designs, which thus suppresses the target-responsive signal change. In addition, the heterogeneity of electrode-surface distributed duplex can further degrade such a response because of the hybridized pairs lying-down (Murphy et al., 2009; Josephs and Ye, 2013). Of note, the specially designed DNA structured probes, such as stem-loop (Fan et al., 2003), pseudoknot (Xiao et al., 2007b) and triplex (Idili et al., 2014), limit the range of measurable target sequences because of the specific requirement to maintain the structural robust and functional configuration. These problems hinder the further application of the structurally switched E-DNA sensor.

Inspired by the classic E-DNA stem-loop conformation (Fan et al., 2003), we herein report a semiduplex DNA structured probe that harbors an unhybridized domain acting as a toehold to trigger strand displacement reaction (SDR) (Zhang and Winfree, 2009), through which the influence of the terminal electroactive reporter is minimized upon hybridization with its complementary sequence. This toehold mediated E-DNA (tE-DNA) sensor is composed of a prehybridized stem-toehold probe, akin to "split" stem-loop strand. One strand of the probe anchors on the interrogating gold electrode surface via Au-S chemistry, and the other strand brings its terminally linked redox molecule (methylene blue, MB) close to the electrode surface for signaling. Such a structure is able to make the toehold domain exposed to an opposite direction. In the presence of target DNA, the toehold fuels a rapid SDR (10 min) with excellent selectivity against even a single-mismatch sequence ascribed to the inherent high selectivity and reaction dynamics of toehold. Additionally, such a facile design renders tE-DNA sensor a high sensitivity (sub-picomolar level) because of the complete release of the signaling strand. As compared to the SNP-oriented locked nucleic acid (LNA) toehold design (Gao et al., 2014), our tE-DNA sensor focuses on how to eliminate the irremovable signaling molecule in structurally switchable E-DNA sensor, and more importantly, this simple design is compatible with homogeneous enzyme-based signal amplification strategy, which can further improve the sensitivity by three orders of magnitude (up to 0.18 fM). This work provides a simple and universal strategy for highly sensitive and selective detection of nucleic acids directly in human serum.

2. Experimental methods

2.1. Materials

All oligonucleotides (Table S1) were synthesized and purified by Sangon Inc. (Shanghai, China). Capture probe 1 (CP1) is thiolated with a-$(CH_2)_6$-spacer at the 5′ end. Target DNA 1 (T1) is a 26-base sequence that contains a perfectly complementary sequence to CP1. Signal probe 1 (MB1) is tailed with methylene blue (MB) at the 3′ end. One-mismatch (1 M), two-mismatch (2 M) and three-mismatch (3 M) sequences are the mutated counterparts of T1, which contains single-nucleotide, two-nucleotide and three-nucleotide mismatch to CP1, respectively. The noncomplementary DNA (NC) is a random sequence that is noncognate to T1. Capture probe 2 (CP2) is thiolated at the 3′ end with a-$(CH_2)_6$-spacer. Signal probe 2 (MB2) is terminated with MB at the 5′ end. Target DNA 2 (T^2) is a sequence with hot mutation spots of a breast cancer gene, BRCA1. Exonuclease III (Exo III) was purchased from New England Biolabs Co. Ltd. (Beijing, China). Health human serum was provided by the affiliated hospital of Hubei University of Chinese Medicine (Wuhan, China). Other reagents and buffers are listed in the supporting information (SI).

2.2. Preparation of the sensor

The detailed experimental procedure can be found in previous literature (Zhang et al., 2007) and the SI. Briefly, 5 μL of CP1 (5′ SH terminal) at appropriate concentrations were dropped on the electrode for overnight at room temperature to form self-assembled monolayers (SAMs). The surface probe density could be modulated by varying the assembly concentration of capture probes. The DNA modified electrodes were subsequently treated with 2 mM MCH for 1 h to fill the unoccupied region and thus assist the SAMs to adopt a favorable interfacial orientation. After that, the functional electrodes were rinsed with Milli-Q water and dried with nitrogen for subsequent hybridization. Signal probes of the corresponding concentration were added to the modified electrodes, allowing for CP1-MB1 binding at 37 °C in a hybridization oven (UVP, HB-1000) with constant temperature and humidity for 40 min in hybridization buffer. Prior to square wave voltammetry (SWV) measurement, the electrodes were extensively rinsed with washing buffer and dried under a stream of nitrogen.

2.3. Toehold mediated SDR and enzymatic amplification

In the first design, different concentrations of T1 were dropped onto the well-prepared functional electrodes with toehold probe to trigger a displacement reaction. After 20 min incubation at room temperature, the electrodes were rinsed thoroughly using washing buffer, 10 mM phosphate buffered saline (PBS, pH 7.4). Then, the displaced strands (MB1) were removed from electrode surface and followed by SWV measurement. Exo III was introduced into the second design, where electrodes were decorated with another toehold probe formed by CP2 and MB2. Prior to measurement, diverse concentrations of T2 coexisted with 1 unit/μL Exo III, were incubated in reaction buffer (20 mM Tris–HCl containing 20 mM $MgCl_2$ and 50 mM NaCl, pH 8.0) for 20 min at 37 °C. Then, the resulting electrode was thoroughly rinsed again for subsequent SWV measurements as previously described.

2.4. Electrochemical measurements

All electrochemical measurements were performed with a CHI660D electrochemical workstation (CH Instruments Inc., Austin, TX). A conventional three-electrode configuration was employed all through the experiment, which comprised a gold working electrode, a platinum wire auxiliary electrode, and an Ag/AgCl reference electrode. SWV measurements were performed by scanning the potential from −0.4 V to −0.1 V in 20 mM Tris–HCl buffer (20 mM $MgCl_2$ and 50 mM NaCl, pH 7.4) with a step potential of 4 mV, a frequency of 25 Hz, and an amplitude of 25 mV. CV and electrochemical impedence spectroscopy (EIS) were carried out in 0.01 M PBS containing 0.1 M KCl and 5 mM $[Fe(CN)_6]^{3-/4-}$, with the potential window from −0.2 to 0.6 V under a scan rate of 0.1 V/s and a bias potential (0.224 V), frequency range (0.1 Hz to 10 kHz), amplitude (5 mV), respectively. Prior to measurements, the electrolyte solution should be completely purged with high purity nitrogen for 15 min, to avoid the interference from the reduction of oxygen.

3. Results and discussions

3.1. Sensor design and signaling mechanism

As demonstrated in Fig. 1A, the irremovable redox labels and the lying-down orientation of electrode surface-bound DNA probes would lead to signal degradation (Josephs and Ye, 2013; Xia et al., 2010). For example, the uprightly oriented duplex complex with a top redox molecule on electrode surface can also produce Faradaic current, and even higher in the "supersandwich" structure (Xia et al., 2010). To address this issue, we here present a highly sensitive E-DNA sensor using a simple pre-hybridized semiduplex probe with a toehold domain (akin to a nicked "loop") inspired by the stem-loop structure (Fig. 1B). In the presence of target sequence, the toehold triggers a rapid SDR by forming a toehold-target duplex complex and releases the signaling strand that is covalently linked with a redox MB. Thus, a larger, readily measurable signal change can be observed (Fig. 1B). In contrast to the classic stem-loop E-DNA sensor (Fan et al., 2003), such a binding-release responsive mechanism via complete removal of signaling probe can greatly improve the sensor's sensitivity. Interestingly, in the presence of the mutant sequence, the toehold will suppress the SDR because of its inherent high discrimination ability to single-base mismatch (Fig. 1B) (Khodakov et al., 2013), and thus a high Faradaic current signal is generated due to the original probe design bringing the electroactive reporter, MB, close enough to the interrogating electrode surface (Fan et al., 2003). More importantly, such a simple design is compatible with the next signal amplification technology. By incorporation of enzyme-mediated target recycling, the sensitivity of this sensor can be further enhanced (Fig. 6A), which is crucial significant in measuring low abundance of target sequences in complex biofluids.

3.2. Optimization of the sensor

EIS was first employed to characterize a step-by-step construction of the sensing interface by using the redox pair of [Fe $(CN)_6]^{3-/4-}$ (Fan et al., 2012). As showed in Fig. 2Aa, no impedance was observed for the bare gold electrode, reflecting the barrier-free diffusion of $[Fe(CN)_6]^{3-/4-}$ to the electrode surface. Also, we observed a pair of well-defined, quasi-reversible redox peaks (CV) bearing the maximum current intensity (Fig. S1a). After immobilization of CP1/MCH on the sensing interface, the interfacial electronic resistance increased significantly. This is caused by strong electrostatic repulsion between the negatively charged phosphate backbone of DNA probes and the same negatively charged $[Fe(CN)_6]^{3-/4-}$, making the indicator difficult to approach the electrode surface (Fig. 2Ab, Fig. S1b). Similarly, a significant decrease in redox currents and an increase in peak separation were observed (Fig. S1), which also confirmed the results. Subsequent hybridization with the signaling strand further improved the electrochemical impedance (Fig. 2Ac), because the absolute amount of electrode surface-confined DNA increased with concomitant enhanced electrostatic repulsion. This newly formed duplex brought the redox MB close to the interrogating electrode surface, and thus a high Faradaic current signal was produced via SWV readout (Fig. 2B). In the presence of the complementary target sequence (10 nM), a high-efficient SDR occurred. This released the signaling probe to the solution at a 1:1 ratio (Fig. 2Ad), leading to a large signal change (Fig. 2B). These results reveal the successful fabrication of the toehold-mediated sensing interface and demonstrate its great potential in sensitive detection of target sequences.

To achieve optimal performance of our tE-DNA sensor, we emphatically investigated two critical parameters, including CP1 to MB1 ratio (C_{CP}/C_{MB}) (SI) and reaction time. As demonstrated in Fig. 2C, while 1 μM target DNA was incubated for 10 min, the signal change first increased along with the ratio across the range of 1:0.5 to 1:3, and then appeared stable even at the ratio of 1:4, indicating a saturated dynamic hybridization at 1:3. Given the cost (MB probe is relatively expensive) and the minimal discrepancy of signal change between 1:2 and 1:3, we chose 1:2 as the optimal surface probe ratio in the next assay. Consistent with the previous report, the assembly concentration of capture probe here was fixed

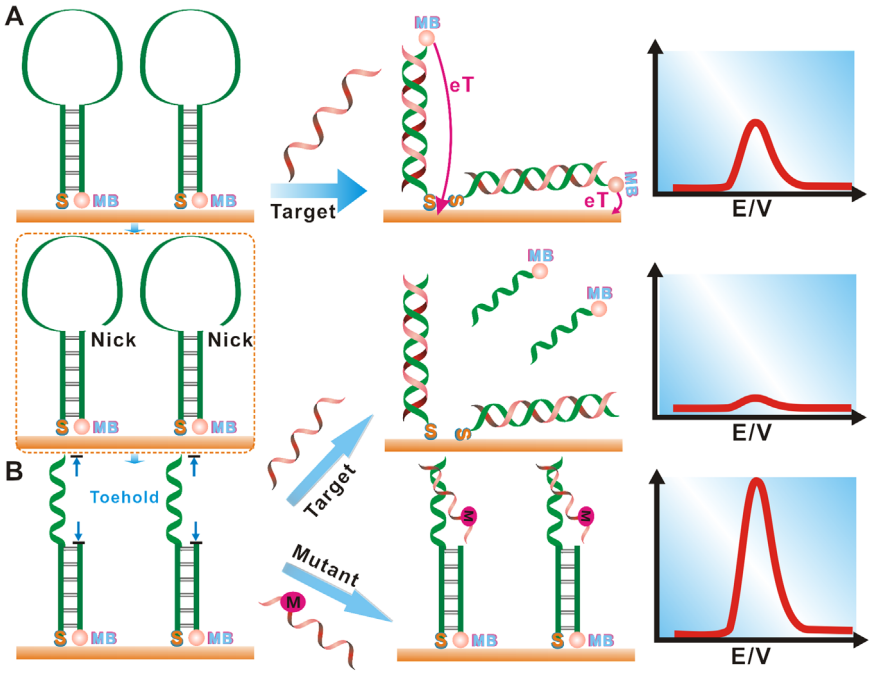

Fig. 1. Schematic representation of the tE-DNA sensor evolved from the classic stem-loop structured E-DNA sensor. (A) The classic stem-loop structured E-DNA sensor with the possible signaling from either upright or lying-down MB-tethered duplex, which can suppress the target-responsive signals. (B) A nicked stem-loop (dot-line box) inspired semiduplex probe with a protruding toehold was employed to measure the complementary oligonucleotides and the mutant sequences, respectively.

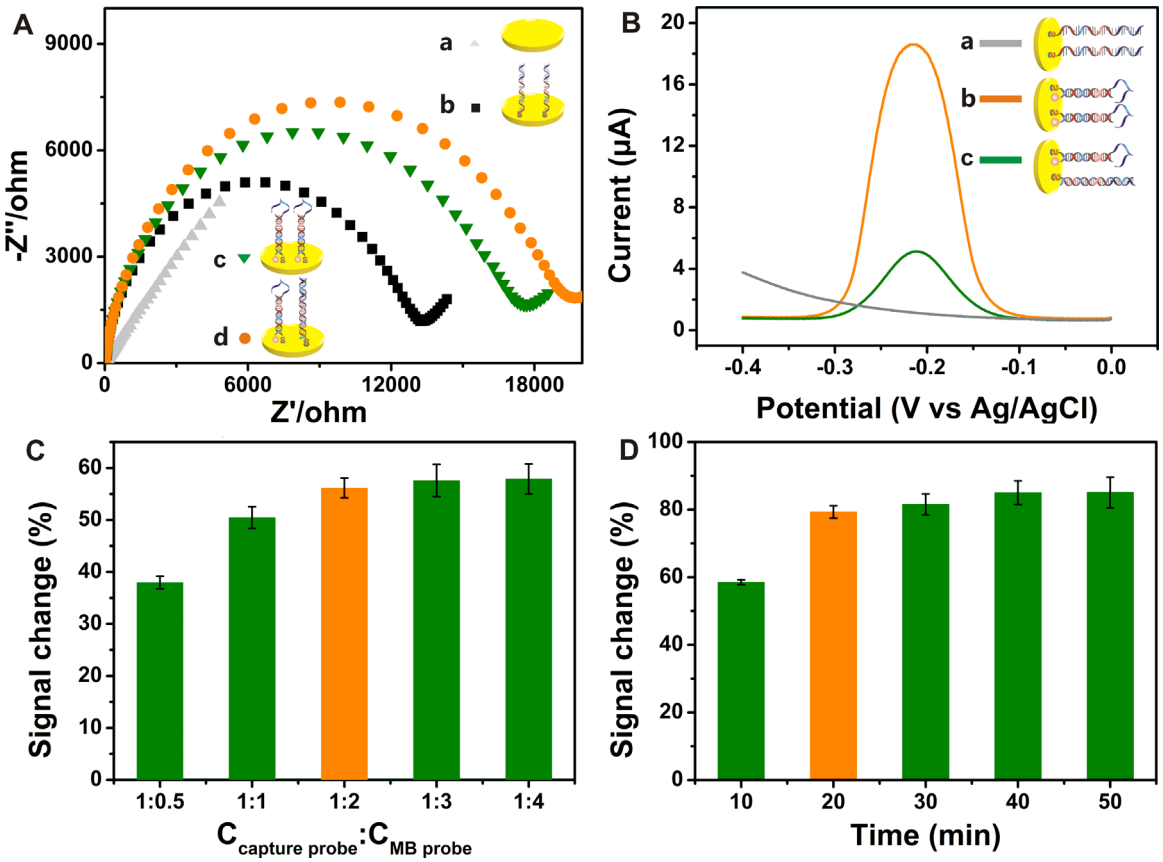

Fig. 2. (A) EIS (Nyquist plots) of a) bare gold electrode, b) CP1/MCH, c) CP1/MB1, and d) CP1/T. (B) SWV of a) CP1/MCH, b) CP1/MB1, and c) CP1/T (1 μM T). (C) The optimization of $C_{capture\ probe}/C_{MB\ probe}$ to maximize the target-responsive signal change (defined as $(I_0\text{-}I_{Target}/I_0)\times 100\%$). The orange column indicates the optimal ratio (10 min incubation). (D) Comparison of the signal change varying with time (i.e., 10, 20, 30, 40, 50 min) of toehold mediated SDR (1 μM T). The orange column indicates the optimal time. Error bars represent standard deviations of measurements (n=3).

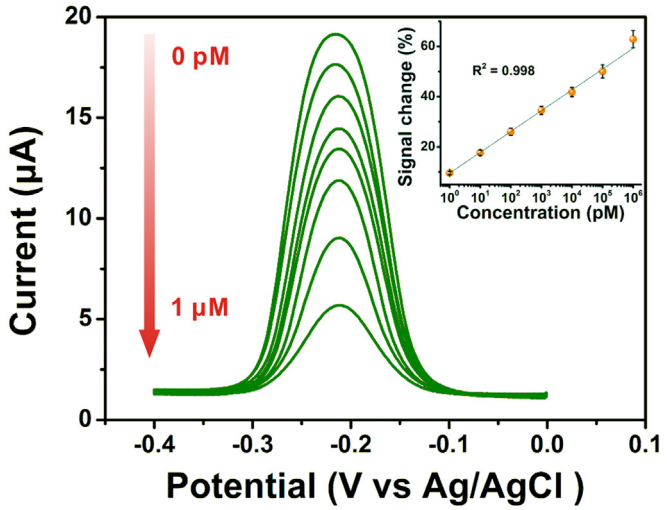

Fig. 3. Typical SWV curves of electrode surface-tethered toehold probes response to target sequence at a series of concentrations, from top to down (red arrow): 0 pM, 1 pM, 10 pM, 100 pM, 1 nM, 10 nM, 100 nM, and 1 μM. Logarithmic plot (inset) of signal change versus target sequence concentrations (from 1 pM to 1 μM). Error bars represent standard deviations of measurements (n=3). (For interpretation of the references to color in this figure legend, the reader is referred to the web version of this article.)

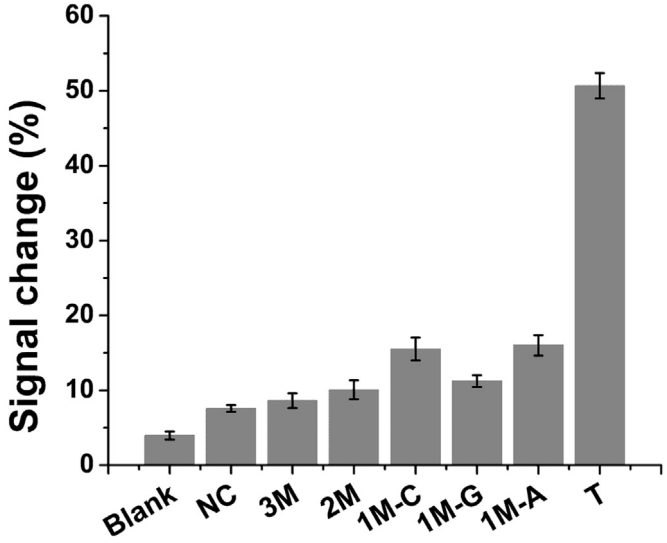

Fig. 4. Selectivity investigation of the tE-DNA sensor for diverse DNA sequences, including blank, NC, 3 M, 2 M, 1 M-(C, G, A) and Target. The concentration of the perfectly complementary T is 100 nM, and that of the other four sequences (i.e., NC, 1 M, 2 M, 3 M) is identical at 200 nM. Error bars represent standard deviations of measurements (n=3).

at 1 μM, which renders a more favorable probe orientation (Yang et al., 2014a).

We then investigated the toehold mediated reaction time to further improve the performance of this sensor. As shown in Fig. 2D, a gradual increase of the signal change occurred along with the elongation of SDR time spanned from 10 min to 50 min, in the presence of 1 μM target DNA and C_{CP}/C_{MB} of 1:2 (C_{CP}=1 μM, C_{MB}=2 μM). Of note, the increasing amplitude of signal reduction slowed down over a reaction time of 20 min. However, prior to

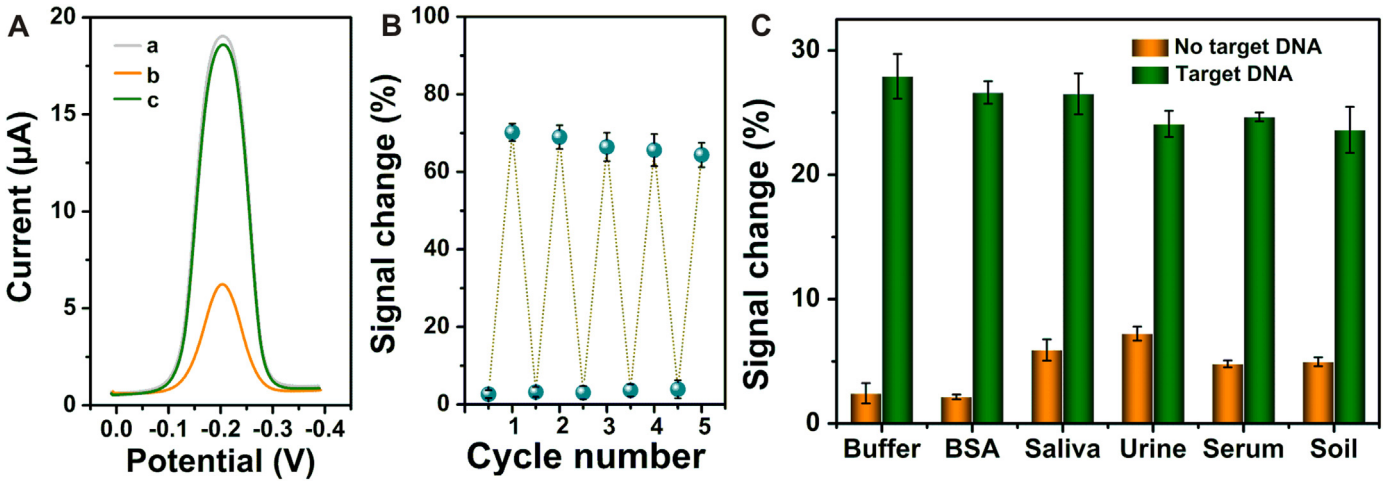

Fig. 5. (A) SWV responses of the regenerated tE-DNA sensor. Upon assembly of toehold probe on the interrogating electrode, a well-defined peak current occurred (curve a). In the presence of target sequence (1 μM), the peak current decreased dramatically (curve b). After regeneration, the current recovered 97.7% of the original current (curve c). (B) Reusability of our tE-DNA sensor over five cycles. (C) Signal change of SWV responses for the tE-DNA sensing in buffer and other interfering matrices. Error bars represent standard deviations of measurements (n=3).

that, the signal variation was relatively intense. It is probably due to the highly frequent collisions between toehold and freely diffused target sequence, which enables a high-efficient SDR in the primary reaction period. With the ongoing depletion of target DNA, the reaction efficiency gradually declined, indicating that reaction equilibrium achieved after 20 min. The reaction time was thus fixed at 20 min, although ~ 60% of signal change (equal to 75% of that at 50 min) could be realized within 10 min.

3.3. Sensitive detection of target DNA

We then employed the optimized tE-DNA sensor to challenge with a series of complementary DNA concentrations ranging from 1 pM to 1 μM. As showed in Fig. 3, the SWV peak current gradually decreased along with increase of target DNA concentrations, suggesting an obvious concentration-dependent signal response. A calibration curve was demonstrated for quantitative analysis of target sequence (Fig. 3 inset), in which the signal reduction ratio was logarithmically related to the concentration of target DNA, spanning a response range of 6 orders of magnitude, from 1 pM to 1 μM. The regression equation is expressed as $s=0.08 \lg c+0.10$, (s is the signal change ratio and c is the concentration of the target DNA), with a correlation coefficient value (R^2) of 0.998. The detection limit of 0.2 pM could be estimated using $3\sigma/S$ (σ is standard deviation of the blank signal and S is the slope of the fit line in Fig. 3 inset). Such a low detection limit for a 1:1 input-output sensor is comparable to or even more sensitive than that of other structural responsive E-DNA sensors and methods involved enzyme-based target recycling or complicated signal amplification strategies (Fan et al., 2003; Xiao et al., 2006, 2007b; Xuan et al., 2012). This is probably attributed to the high-efficient SDR, in which the rigid duplex stem structure renders the toehold an "upright" orientation for enhanced molecular recognition, and the complete release of signaling probe to suppress the post-responsive interfering signals. To better show the advantages of this tE-DNA sensor, the associated performance parameters (e.g., responsive strategy, detection limit, range and regeneration) have been compared with those obtained by other similar strategies and listed in Table S2.

3.4. Selectivity of tE-DNA sensor

Due to the significance of sensor selectivity, especially in SNP assays, we next evaluated the discrimination capability of our tE-DNA sensor by using a series of control sequences, comprising single-base (1M-G, A, C), two-base (2 M), three-base (3 M) mismatched sequences and noncognate DNA sequence (NC) as targets. We found all the mismatched sequences could be readily distinguished from the perfectly complementary DNA, in which the concentration of the perfectly matched sequence (100 nM) is halved to that of the mismatched counterparts (200 nM) (Fig. 4). It was noticed that only the fully matched DNA exhibited prominent signal change, while the alteration caused by all the other mismatched oligonucleotides was negligible. Such an excellent selectivity of the sensor may benefit from the toehold design, in which a protruded functional domain (7-nt in length), serving as a fueling probe to trigger SDR, possesses an outstanding ability capable of differentiating single-base mismatch sequence (Wang et al., 2012). It should be noted that our novel sensor can easily distinguish a single-base mismatch DNA at room temperature without relying on stringent thermal control. It is anticipated that the selectivity might be further improved by using highly specific LNA or peptide nucleic acid (PNA) as capture probes, and such an excellent selectivity combined with the sub-picomolar sensitivity will make our novel sensor more suitable for SNP analysis (Gao et al., 2014).

3.5. Regeneration, stability and anti-interference of tE-DNA sensor

Besides sensitivity and selectivity, regenerability is another important feature for biosensors in practical applications. We found the tE-DNA sensor could be easily regenerated by rinsing the sensor in urea (8 M) for 5 min at room temperature to denature the hybridized duplex, and rehybridizing with the target DNA sequence. After regeneration, the Faradaic current recovered 97.7% of the original current signal (Fig. 5A). By repeating this regeneration process for 5 cycles, our sensor still retained its original hybridization efficiency with a standard deviation of 2.4% for the measurements (Fig. 5B).

In addition, our tE-DNA sensor demonstrated high stability (RSD=4.7%) in the repeated SWV readout of the target-responsive currents, which was performed every 24 h for a week storage at 4 °C (Fig. S2). After storage of 7 days, the sensor retained 89% of its initial response, meaning that the sensor has a good stability.

To further demonstrate the superiority of the tE-DNA sensor, it was challenged directly in complex samples by spiking DNA targets (100 pM) in multiple matrices, such as 2.5% BSA, 4% soil, 50%

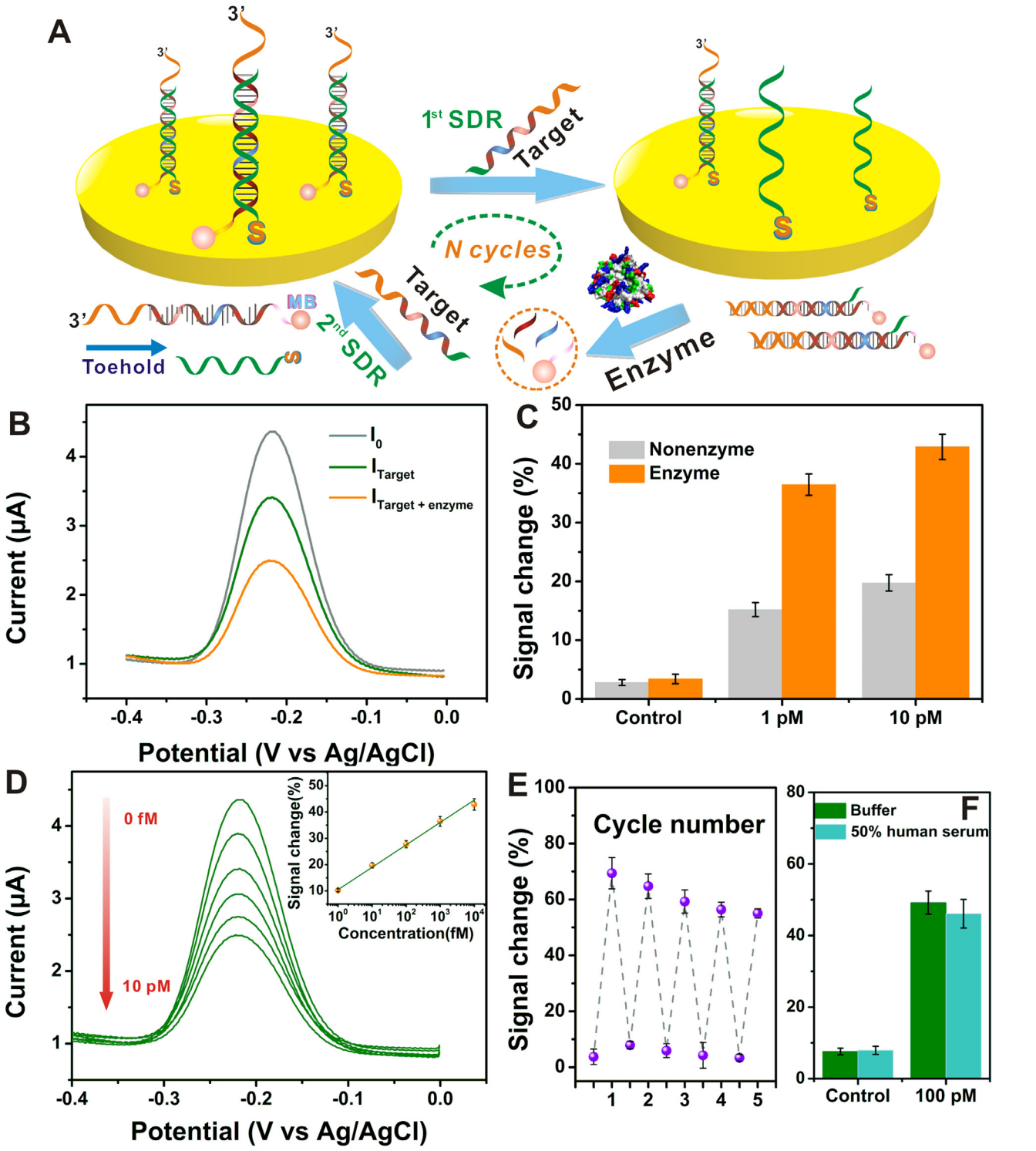

Fig. 6. Enzyme mediated ultrasensitive tE-DNA sensor. (A) Scheme of Exo III based cyclic signal amplification. (B) SWV curves of tE-DNA sensor in response to the blank (gray line), target sequence (green line) and enzyme solution containing targets (orange line). (C) Comparison of signal change between the Exo III mediated signal amplification and the nonenzymatic 1:1 displacement reaction. (D) Typical SWV curves of tE-DNA sensor in response to a series of target concentrations, from top (0 fM) to down (10 pM) (red arrow). The green line (inset) represents the linear relationship between the signal change and the logarithm of target DNA concentrations. (*E*) Reusability of our enzyme mediated tE-DNA sensor over five cycles. (F) Signal change of SWV responses for the enzyme mediated tE-DNA sensing in buffer and 50% human serum. Error bars represent standard deviations of measurements (n=3). (For interpretation of the references to color in this figure legend, the reader is referred to the web version of this article.)

human saliva, urine and serum. Fig. 5C showed a negligible signal change as the functionalized sensor was incubated either in buffered saline or in the interfering substances, despite its extremely complex and multicomponent nature that might degrade the performance of the sensor. Such impressive anti-interference is mainly contributed by the excellent base pairing ability of sequence-specific hybridization and the toehold-mediated high-efficient strand displacement.

3.6. Enzyme-mediated Ultrasensitive detection of tumor DNA

Interestingly, the simple design strategy of the tE-DNA sensor could be easily extended to couple with enzyme mediated target-recycling amplification to further improve the sensor's sensitivity. As schemed in Fig. 6A, in the presence of target sequence, a pre-hybridized "stem-toehold" DNA structured probe well-arranged on the heterogeneous interrogating electrode can trigger a SDR to form a toehold-target duplex (3′ toehold domain and MB reporter coexist on the signaling probe in this design). The duplex is then released into homogeneous solution and digested by Exo III with a higher efficiency than that on heterogeneous surface (Xuan et al., 2012). It should be noted that Exo III catalyzes the stepwise removal of mononucleotides from 3′ terminus of the released double-stranded DNA, and its preferred substrates are blunt or recessed 3′ termini (Zuo et al., 2010). Moreover, because the spacer is needed to ensure blunt 3′ terminus, the terminal MB reporter is relatively distant from the interrogating surface in contrast to the design in original tE-DNA sensor, thus achieving a relative low background signal (Fig. S3). After complete digestion of the toehold strand from toehold-target duplex, the signaling molecule of MB is freed, leading to considerable signal variation. Meanwhile the left target strand will rejoin the target-responsive SDR until the depletion of the electrode surface-attached toehold probes (Fig. 6A). Finally, a significantly enlarged signal change (input 1 and output *N*) will be achieved.

After successful construction of the enzyme-oriented nucleic acid sensing interface (Fig. S4), the introduction of Exo III could significantly enhance the Faradaic current signal change from 0.95 μA (I_0-I_{Target}) of nonenzymatic tE-DNA sensor to 1.86 μA (I_0-$I_{Target+enzyme}$), nearly 200% increase in the detection of 1 pM breast cancer gene sequence (T^2, Table S1) (Fig. 6B). Fig. 6C clearly demonstrated the results of enzymatic signal amplification in measuring target gene sequence at 1 pM and 10 pM, respectively. In both cases, the response increased by more than two-fold over that of nonenzymatic sensor, suggesting a compatible and attractive catalytic ability of Exo III toward our sensor. Next, this enzyme mediated tE-DNA sensor was challenged with gradient concentrations, ranging from 1 fM to 10 pM of the target gene sequence. The sensor showed concentration-dependent signal response (Fig. 6D), and a favorable linear relationship was obtained with a regression equation expressed as $s=8.5\ \lg c+10.5$, with a correlation coefficient value (R^2) of 0.996 (Fig. 6D inset). This novel sensor achieved a detection limit of 0.18 fM (estimated with 3 times the standard deviation of the blank), which is lower than that of nonenzymatic tE-DNA sensor (0.2 pM) by three orders of magnitude. This unique sensor also exhibited impressive regenerability of sensing interface. As displayed in Fig. 6E, the signal change was reduced less than 15%, after consecutive regeneration of 5 times by simple exposure to urea (8 M) for denaturation. Such a strong regenerating ability is mainly ascribed to the facile target-responsive binding-and-release design. Of note, this enzyme-based tE-DNA sensor could realize an accurate measurement of target sequence even in complex 50% human serum with negligible signal degradation (Fig. 6F). All these advantages, especially the ultrahigh sensitivity, enable this sensor to be an appealing sensing platform for the bioassay of low-abundance biomarkers.

4. Conclusions

In summary, we have tailor-engineered a tE-DNA sensor for highly sensitive, label-free and sequence-specific electrochemical readout of target DNA (including breast cancer gene sequence) in human serum using a toehold-contained semiduplex structured probe. This unique sensing mechanism, upon target-responsive complete elimination of signaling probe, appears to be more efficient than the traditional E-DNA sensor requiring an exquisite design of structurally folded or switchable probe, and competes well with them in terms of sensitivity and selectivity. Beyond that, this novel sensor has several impressive advantages. First, such a design facilitates the probe-target hybridization via the protruded toehold domain (as compared to that of stem-loop probe, in particular those with long stem), allowing a complete release of the signaling strand to enhance the target-responsive signal change. Meanwhile, such a mechanism can circumvent the signal degradation that stems from the orientation heterogeneity of electrode surface-confined DNA probe. Second, toehold endows this sensor not only an outstanding discriminating capability between wild-type and mutant sequence, but also high hybridization efficiency. More importantly, toehold triggered SDR is easily extended to cooperate with enzyme-mediated target recycling for further enhancement of sensor's sensitivity. Third, our novel sensor is easily regenerated, and can be employed directly in human serum (50%) with minimal signal degradation. By synergizing with other emerging technologies, such as nanostructured electrode-based electrocatalysis (Lapierre et al., 2003), electric field enhanced hybridization and single-step delivery coupled microscale electrochemical sensing array (Kaiser and Rant, 2010; Yang et al., 2014b), this unique DNA sensor will be a more promising nucleic acid readout strategy for clinical diagnostics.

Acknowledgements

This work was supported by the National Natural Science Foundation of China (21305034, 21275040 and 21475034).

Appendix A. Supporting information

Supplementary data associated with this article can be found in the online version at doi:10.1016/j.bios.2016.03.054.

References

Anker, J.N., Hall, W.P., Lyandres, O., Shah, N.C., Zhao, J., Van Duyne, R.P., 2008. Nat. Mater. 7, 442–453.
Cai, B., Huang, L., Zhang, H., Sun, Z., Zhang, Z., Zhang, G.-J., 2015. Biosens. Bioelectron. 74, 329–334.
Cai, B., Wang, S., Huang, L., Ning, Y., Zhang, Z., Zhang, G.-J., 2014. ACS Nano 8, 2632–2638.
Chung, H.J., Castro, C.M., Im, H., Lee, H., Weissleder, R., 2013. Nat. Nanotechnol. 8, 369–375.
Drummond, T.G., Hill, M.G., Barton, J.K., 2003. Nat. Biotechnol. 21, 1192–1199.
Fan, C., Plaxco, K.W., Heeger, A.J., 2003. Proc. Natl. Acad. Sci. USA 100, 9134–9137.
Fan, Q., Zhao, J., Li, H., Zhu, L., Li, G., 2012. Biosens. Bioelectron. 33, 211–215.
Ferguson, B.S., Buchsbaum, S.F., Swensen, J.S., Hsieh, K., Lou, X., Soh, H.T., 2009. Anal. Chem. 81, 6503–6508.
Ferguson, B.S., Buchsbaum, S.F., Wu, T.-T., Hsieh, K., Xiao, Y., Sun, R., Soh, H.T., 2011. J. Am. Chem. Soc. 133, 9129–9135.
Gao, Z.F., Ling, Y., Lu, L., Chen, N.Y., Luo, H.Q., Li, N.B., 2014. Anal. Chem. 86, 2543–2548.
Giljohann, D.A., Mirkin, C.A., 2009. Nature 462, 461–464.
Hong, J.W., Studer, V., Hang, G., Anderson, W.F., Quake, S.R., 2004. Nat. Biotechnol. 22, 435–439.
Hsieh, K., Ferguson, B.S., Eisenstein, M., Plaxco, K.W., Soh, H.T., 2015. Acc. Chem. Res. 48, 911–920.
Idili, A., Amodio, A., Vidonis, M., Feinberg-Somerson, J., Castronovo, M., Ricci, F., 2014. Anal. Chem. 86, 9013–9019.
Josephs, E.A., Ye, T., 2013. ACS Nano 7, 3653–3660.
Kaiser, W., Rant, U., 2010. J. Am. Chem. Soc. 132, 7935–7945.
Khodakov, D.A., Khodakova, A.S., Linacre, A., Ellis, A.V., 2013. J. Am. Chem. Soc. 135, 5612–5619.
Lapierre, M.A., O'Keefe, M., Taft, B.J., Kelley, S.O., 2003. Anal. Chem. 75, 6327–6333.
Liong, M., Hoang, A.N., Chung, J., Gural, N., Ford, C.B., Min, C., Shah, R.R., Ahmad, R., Fernandez-Suarez, M., Fortune, S.M., Toner, M., Lee, H., Weissleder, R., 2013. Nat. Commun. 4, 1752.

Lu, Y., Peng, S., Luo, D., Lal, A., 2011. Nat. Commun. 2, 578.
Lubin, A.A., Plaxco, K.W., 2010. Acc. Chem. Res. 43, 496–505.
Murphy, J.N., Cheng, A.K.H., Yu, H.-Z., Bizzotto, D., 2009. J. Am. Chem. Soc. 131, 4042–4050.
Ricci, F., Lai, R.Y., Plaxco, K.W., 2007. Chem. Commun., 3768–3770.
Soleymani, L., Fang, Z., Sargent, E.H., Kelley, S.O., 2009. Nat. Nanotechnol. 4, 844–848.
Tokel, O., Inci, F., Demirci, U., 2014. Chem. Rev. 114, 5728–5752.
Wang, D., Tang, W., Wu, X., Wang, X., Chen, G., Chen, Q., Li, N., Liu, F., 2012. Anal. Chem. 84, 7008–7014.
Wu, Y., Lai, R.Y., 2013. Chem. Commun. 49, 3422–3424.
Wu, Y., Lai, R.Y., 2014. Anal. Chem. 86, 8888–8895.
Xia, F., White, R.J., Zuo, X., Patterson, A., Xiao, Y., Kang, D., Gong, X., Plaxco, K.W., Heeger, A.J., 2010. J. Am. Chem. Soc. 132, 14346–14348.
Xiao, Y., Lai, R.Y., Plaxco, K.W., 2007a. Nat. Protoc. 2, 2875–2880.
Xiao, Y., Lubin, A.A., Baker, B.R., Plaxco, K.W., Heeger, A.J., 2006. Proc. Natl. Acad. Sci. USA 103, 16677–16680.
Xiao, Y., Piorek, B.D., Plaxco, K.W., Heeger, A.J., 2005. J. Am. Chem. Soc. 127, 17990–17991.
Xiao, Y., Qu, X., Plaxco, K.W., Heeger, A.J., 2007b. J. Am. Chem. Soc. 129, 11896–11897.
Xuan, F., Luo, X., Hsing, I.M., 2012. Anal. Chem. 84, 5216–5220.
Yang, F., Yang, X., Wang, Y., Qin, Y., Liu, X., Yan, X., Zou, K., Ning, Y., Zhang, G.-J., 2014a. Anal. Chem. 86, 11905–11912.
Yang, F., Zhang, G.-J., 2014. Rev. Anal. Chem. 33, 95–110.
Yang, F., Zuo, X., Li, Z., Deng, W., Shi, J., Zhang, G., Huang, Q., Song, S., Fan, C., 2014b. Adv. Mater. 26, 4671–4676.
Zhang, D.Y., Winfree, E., 2009. J. Am. Chem. Soc. 131, 17303–17314.
Zhang, J., Song, S., Wang, L., Pan, D., Fan, C., 2007. Nat. Protoc. 2, 2888–2895.
Zhu, C., Yang, G., Li, H., Du, D., Lin, Y., 2014. Anal. Chem. 87, 230–249.
Zuo, X., Xia, F., Xiao, Y., Plaxco, K.W., 2010. J. Am. Chem. Soc. 132, 1816–1818.